Indian Journal of Pure & Applied Physics
Vol. 57, March 2019, pp. 157-165

Synthesis of nanostructured thin films for resolution and diffraction/ camera length calibration of transmission electron microscopes

Sukhvir Singh*, Dinesh Singh & Manjri Singh

CSIR- National Physical laboratory, New Delhi 110 012, India

Received 12 June 2018; accepted 31 October 2018

Transmission electron microscope (TEM) is one of the highly sophisticated, sensitive and accurate tool for carrying out microstructural detailed investigations of the materials in terms of their crystallographic structure, lattice imaging, phase identification, variety of defects present, particle size and shape analysis, *etc.*, at the nano scale level. The accuracy and efficiency of electron microscope depends upon the magnification and resolution of the instrument. Evaporated films of gold, magnesium oxide, and thallium chloride make excellent calibrating substances since they have *d* (interplaner spacing) values accurately determined by *x*-ray diffraction. In the present investigations, preliminary studies on thermally evaporated thin films of high purity tin and silver deposited on KCl substrate and carbon coated Ni/Cu TEM grids under high vacuum conditions (of the order of 10^{-6} torr) have been undertaken. These films have been characterized for particle shape, size, lattice imaging by using TEM, high resolution transmission electron microscope (HRTEM) and selected area electron diffraction (SAED) pattern. The deposition process of nanoparticles has precisely been monitored to get high quality, stable and with repeatable and uniform sized particles. The aim of the study is to optimise the synthesis parameters to deposit uniformly distributed nano size gold particles using thermal evaporation technique which will be further used as a standard sample for the calibration of camera length and resolution of TEM.

Keywords: Microstructural, Resolution, Camera length, Transmission electron microscope

1 Introduction

The testing and calibration of an instrument in routine has become an important factor for scientists and engineers involved in variety of metrological measurements. As per the ISO/IEC/17025 standard recommendations for globally acceptable results, the measurement should be carried out by a standard method accepted internationally/validated method with the help of standard/calibrated instrument or by standard reference material with proper listing of its uncertainty and traceability. The importance for uniform approach of measurement in the estimation of uncertainty and its reporting has attracted metrologists globally.

The transmission electron microscope (TEM) is one of the main instruments for the measurements of linear sizes of nano objects and nano materials. High resolution transmission electron microscopy (HRTEM) has become an indispensable tool for studying the nature of materials at nanoscale. It allows detailed microstructural examination through high resolution and high magnification, in real and reciprocal space imaging to identify phases through selected area electron diffraction pattern, phase transformation, epitaxial growth, various defects, particle shape and size, *etc.*, at nano and sub-nano scale. In crystalline materials the atomic location and lattice arrangement can also be determined by employing HRTEM, which is widely used in the research and development of advanced materials[1]. TEM's point resolution and the resolution in the mode of the scanning transmission electron microscope (STEM-mode) can reach the values of 70–80 pm. A wide range of magnifications (from 50 to 300000 times), which can be achieved in a TEM, result in the necessity of using a number of magnification standards, different in their structure and fabrication methods, for calibration of the TEM magnification. As a rule, different magnification standards are used for different magnification ranges[2]. For a high-resolution TEM (HRTEM) (the microscope magnification exceeds 300000 times), thin cross-sections of single crystals and single-crystalline gold islands are usually used. In this case, the magnification calibration is performed using a lattice-plane spacing of single crystals, such as the single crystals of gold and silver. Aberration correctors and image reconstruction methods[3] have pushed the point

*Corresponding author (E-mail: sukhvirster@gmail.com)

resolution of TEM to about 0.05 nm. With the increasing requirement of HRTEM images, an accurate magnification calibration of TEM becomes more and more critical[4].

Many of the existing magnification standards have several shortcomings. For instance, polystyrene spheres can be subject to radiation damage, as well as contamination. As for replicas of gratings, their sizes can change during the fabrication process, and their edges can turn out to be uneven. Besides, for replicas of gratings, only the average grating periodic certified but the actual distance between neighbouring lines may be different from the certified average[5]. However, the preparation of single crystal silicon reference material is costly and time-consuming, which need to use ion beam milling. Also the electron transparent area of single-crystal silicon is extremely fragile and easily broken. Furthermore, the dislocation density in single-crystal silicon is very large and the strain field induced by dislocation will finally lead to the distortion of HRTEM images[6]. Oxygen absorption will slowly proceed when single-crystal silicon is exposed to air, which also can cause lattice distortion[7,8].

The ability and accuracy of the electron microscope depends on the magnification and the resolution of the microscope. Hence in order to achieve high accuracy measurement results from the electron microscopic examination, a standard specimen is required to calibrate the camera constant, and the magnification of the electron microscope. Two kinds of nanoparticles, *i.e.*, silver nanoparticles and gold nanoparticles have been synthesized. Gold and silver nanoparticles are used as calibration standard due to their easy preparation and good structural stability. However, the main structural feature of gold nanoparticles is five-fold rotational twinning parallel to [1 1 0] axis. As a result of this structure, real gold nanoparticles are intrinsically strained[9].

These nano sized materials are developed by various processes under different conditions and find wide range of practical applications in many technologically important devices. In order to achieve high level of accuracy and efficiency in the measurements of the above mentioned parameters in day to day work for scientific research and development, innovations, calibration of certain parameters of the electron microscope have drawn considerable attention. It is important to mention here that magnification and resolution are interrelated features and are always related to the efficiency of the microscope. Since the characterization of materials under the electron beam inside the microscope is dealing at sub nano scale, it is very important to have the equipment always with extremely high precision.

The testing and calibration of an instrument in routine has become an important factor for scientists and engineers involved in variety of metrological measurements[10]. Conventionally, thin films are deposited either by sputtering or by evaporation in vacuum system. For sputter deposition, the films are usually sputtered from an alloy/compound/element target or by co-sputtering. The composition of the films, however, cannot be continuously varied by sputtering from one single element target and the cost of the co-sputtering apparatus is high. Hence, in the present work, the thermal evaporation deposition technique is preferred as it is easy, economical and less time consuming. Evaporated films of gold, magnesium oxide, and thallium chloride make excellent calibrating substances since they have *d* values accurately determined by *x*-ray diffraction. Before we proceed to the synthesis and characterization of resolution test sample, some basic parameters to be understand as reported in this manuscript.

1.1 Electron beam and specimen interaction

HRTEM is an indispensable tool for nanotechnology research and development. TEM is a very big microscope which uses number of electromagnetic lenses. In the TEM, electrons are emitted by the electron source. A number of optics is used for projecting the electrons on to the samples which is kept near the objective lens. Various types of scattering between electron and atom occur and then a number of lenses are used for magnifying the beam on the florescent screen, shown in Fig. 1 and Fig. 2.

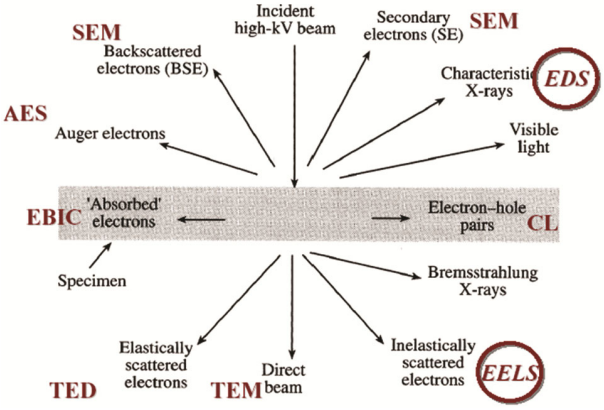

Fig. 1 — Electron beam and specimen interaction.

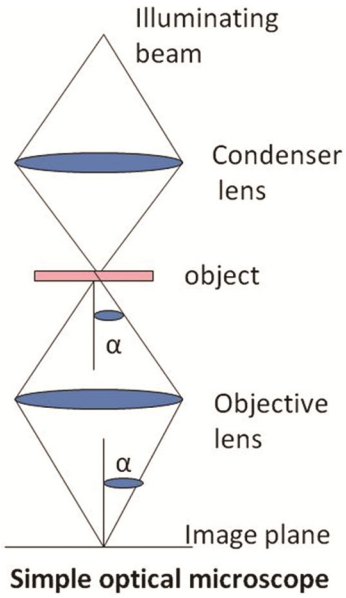

Fig. 2 — Schematic diagram for simple optical microscope.

A TV camera and CCD camera are also used to take picture. The resolution of the instrument depends on many parameters like accelerating voltage, vacuum and coherence of the beam. Thus, TEM is used to understand how the electrons interact with the atom in the sample and matter and various phenomenon occurring there. The sample should be very thin in the range of 100 Å to as much as micron thick. Sample has to be thin so that electron can pass through the sample to the other side. Electron coming with high energies something like 100-300 kV can penetrate all the way through the sample. It is advisable to first understand the crystal structure using the electron microscope. Thus, first diffraction (simple Bragg law type scattering) experiment is carried out. The elastically scattered electron results in diffraction information. And through in-elastically scattered electrons (the electrons that interacted with the atoms so strongly to lose some energy) the identification and position of atoms can be found out. Also some different signal coming out like characteristic X-rays are used for analytical work. All these things can provide us with lot of information about the sample. Now depending upon the crystallinity of sample, one obtains a diffraction pattern.

Specimen interaction is what makes electron microscopy possible. The energetic electrons in the microscope strike the sample and various reactions can occur as shown above. The reactions noted on the top side of the diagram are utilized when examining thick or bulk specimen (SEM) while the reactions on the bottom side are those examined in thin or foil specimens (TEM).

1.2 Resolution and the accelerating voltage of the microscope

The resolution of the microscope is the smallest distance (separation) of two points in the object which may be distinctly reproduced in the image.

$$\text{Resolution} = K\lambda / N_o \sin\alpha \cdot \quad \ldots (1)$$

Where λ is the wavelength of illumination (light or electron beam), N_o is refractive index in object space, α is semi-angle subtended by the object at lens and K is constant.

$N_o \sin\alpha$ is usually called numerical aperture of the lens. Value of K depends on the coherence of the illumination. K = 0.61 in case of light and electron microscopy.

From Eq. (1) it is clear that best resolution can achieved using combination of shortest λ with large numerical aperture. For Light λ = 550 nm and *No* sin α = 1.6, resolving power = 0.2 μm (200 nm).

Thus, smaller the wavelength of the source, higher will be the resolution of the system. In the transmission electron microscopy, much smaller wavelength electrons (0.03 Å) are used instead of photons (λ> 1000 Å).

De-Broglie equation shows that the wavelength of electron is related to their energy E if we ignore relativistic effect we have:

$$\lambda \sim 1.22/(E)^{1/2} \text{ or } \lambda = h/p \quad \ldots (2)$$

where h is the planks constant, p is momentum of the particle.

For the specific case of electron, momentum is usually acquired by falling through a potential difference, V in volts, termed the accelerating voltage. Since energy is conserved,

$$1eV = 1/2\ mv^2 \cdot \quad \ldots (3)$$

$$1eV = p^2/2m \quad \text{or} \quad p^2 = 2meV \quad \text{or} \quad p = (2meV)^{1/2}$$

Thus, the $1eV = 1.602\times10^{-19}$ J is the energy acquired by an electron passing through a potential difference of 1 volts, where e is charge, m is mass and v is velocity.

So, from Eqs (2) and (3):

$$\lambda = h/(2meV)^{1/2} \quad \ldots (4)$$

Since voltage is often very large, the electron can reach the velocity of the light C and the relativistic increase in mass of the electron should be taken into

account. This can easily be done by replacing by the relativistic accelerating voltage Vr given by the relation:

$$Vr = V[1+eV/2m_oC^2]\cdot \quad \ldots (5)$$

where m_o is the mass of the electron.

This correction becomes important for $V > 10^5$ volts

$$\lambda = h/ (2meVr)^{1/2}$$

$$\lambda = h/ [2me\ V[1+eV/2m_oC^2]^{1/2} \quad \ldots (6)$$

Substituting the values of m_o and voltage we can find out the values of wavelengths (Table 1).

1.3 Electron diffraction and diffraction standard- camera length constant

Electron diffraction provides a basis for studying the structure of crystals and thereby identifying materials. Metals tend to give very strong electron diffraction patterns, whereas biological specimens generally diffract quite weakly. Depending on the nature of the specimen, a diffraction pattern usually consists of a series of rings (for specimens consisting of many randomly oriented microcrystals) or a discrete lattice of sharp spots (for specimens with a single, crystalline domain). Each sharp spot in the diffraction pattern is an image of the electron source since the imaging system is set to bring the image of the electron source to the viewing screen. The nominal value of the effective camera length of an electron microscope (EM) operating in the selected area mode is not sufficiently accurate for calculations of lattice spacing. The actual value of camera length must be calibrated at the same accelerating voltage and objective lens setting by reference to a known substance with well-defined diffraction spacing. A normal specimen is evaporated film of aluminium with a thickness of around 31 nm (SAED pattern shown in Fig. 3). Very small crystallite size yields ring patterns suitable for calibration. The specimen is supplied with a list of the principal lattice spacing. Made on a G400, 400 square mesh copper Gilder grid.

Table 1 — Electron properties as a function of accelerating voltages.

Accelerating voltage (kV)	Nonrelativistic wavelength (nm)	Relativistic wavelength (nm)	Mass ($\times m_o$)	Velocity ($\times 10^8$ m/s)
100	0.00386	0.00370	1.196	1.644
120	0.00352	0.00335	1.235	1.759
200	0.00273	0.00251	1.391	2.086
300	0.00223	0.00197	1.587	2.330
400	0.00193	0.00164	1.783	2.484
1000	0.00122	0.00087	2.957	2.823

The camera constant is defined as λL, where L is the camera length (usually expressed in mm; typically L = 300 mm, and λ, an electron wavelength measured in Å). When the camera constant is known, the d spacing in the crystal can be calculated when R is measured. Note that, as the accelerating voltage is decreased (and electron wavelength, λ increases), the scale of the diffraction pattern increases.

If the geometry of the system and wavelength of the electron beam are known exactly, the instrument constant, L, can be derived and spacing in the specimen can be calculated from measurement of the spots or rings in the diffraction pattern. It is difficult to determine the wavelength accurately by experiment (and it may change with time) and it is impractical to measure the high voltage with sufficient accuracy to find the wavelength by calculation.

The only practical method is to calibrate the instrument through the use of a diffracting substance of known structure. Since the instrument constant depends on lens currents and object position, ideally the calibration pattern should be taken at the same time as the unknown.

The calibration is accomplished by taking a diffraction pattern of a specimen whose d values are known, measuring the radial distances of the spots produced by the diffracted beam.

Fig. 3 — An example of SAED pattern of thermally evaporated aluminium film.

Evaporated films of gold, magnesium oxide, and thallium chloride make excellent calibrating substances since they have *d* values accurately determined by X-ray diffraction. Incident electrons that are scattered (deflected from their original path) by atoms in the specimen in an elastic fashion (no loss of energy). These scattered electrons are then transmitted through the remaining portions of the specimen.

All electrons follow Bragg's law and thus are scattered according to $n\lambda=2d\sin\theta$. All incident electrons have the same energy (thus wavelength) and enter the specimen normal to its surface. All incident electrons that are scattered by the same atomic spacing will be scattered by the same angle.

These "similar angle" scattered electrons can be collated using magnetic lenses to form a pattern of spots; each spot corresponding to a specific atomic spacing (a plane). This pattern can then yield information about the orientation, atomic arrangements and phases present in the area being examined.

Electron beam interacts with substances to a far greater extent than in the case of X-rays. In other words the scattering power (diffraction wave amplitude/incident wave amplitude) of electron beams is far greater (10^6 times or more) than that of X-rays. As a result small specimens are able to yield clear diffraction patterns.

That is to say that the film with a thickness of 500 Å (50 nm) or less can be effectively studied by electron beam diffraction. Furthermore electron is used to estimate the orientation of the crystal and the size and shape of the crystallite from the shape and structure of the pattern.

When incident electron waves are scattered by the atoms in a substance, the wave expand spherically from the center of the atom. Moreover, when the specimen is in the crystalline state, having a regular three dimensional arrangement of atoms, a constant phase relationship exists between the waves emitted from the respective atoms.

These waves travel in one direction only and are mutually coherent. This is known as “Bragg’s reflection”. The electron waves are reflected by the atomic net planes. If the path difference, $2d\sin\theta$ (shown by the thick lines in the figure) is equal to $n\lambda$, where n is an integer, and λ is the wavelength, the waves reflected at successive planes will be in phase. Thus, Equation $2d\sin\theta=n\lambda$ is obtained.

When an electron microscope is used as an electron diffraction apparatus, the equation changes to:

$$d2\theta = \lambda$$

$$\lambda/d = 2\theta \cdot \quad \ldots (7)$$

where n=1 and $\sin\theta = \theta$, Bragg angle for high velocity electron beam is very small.

Here, O is the center spot, H is the diffraction spot (or a point on the ring), and L is the distance between the crystal and the film (camera length), r is the distance between O and H. Here, $L\lambda$ is known as camera constant (Fig. 4). Now from diffraction pattern the final equation can be expressed as follows:

$r/L = \tan2\theta$ (Here, $\tan2\theta = 2\theta$ when θ is very small)

$$r/L=2\theta \quad \ldots (8)$$

From Eqs (7) and (8):

$$rd=L\lambda \quad \cdot\ldots (9)$$

Knowing the values of r, L and λ, we can calculate interplaner spacing d.

2 Experimental Details

Thermal evaporation technique is easy and economical for depositing good quality nano-structured thin films. In this method, high purity element was evaporated by resistive heating from a molybdenum boat in high vacuum (in the range of 10^{-6} mbar) system Model VT-ACG-03. In this technique, properties of thin films strongly depend on the processing parameters like substrate temperature, vacuum inside the chamber, evaporation rate, distance between substrate and the source material, boat current etc. during the evaporation[11,12]. Rates of evaporation are dependent upon the temperature of

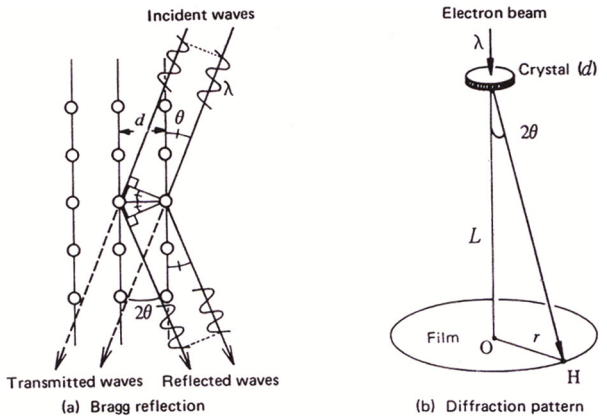

Fig. 4 — Schematic diagram of electron diffraction.

source. The rate of evaporation G from a surface at a temperature T is given by the Langmuir expression $G = p\ (M/2\pi RT)^{½}$ where, p is the vapour pressure of the material at temperature T and M the molecular weight and R is the gas constant per mole. High purity (99.999% pure) gold was used as a source material to deposit its thin films. The glass pieces used as substrates were first cleaned by warm dilute nitric acid (1:10) and mild detergent (soap solution). The glass substrates were then thoroughly cleaned with doubled distilled water in an ultrasonic cleaner and finally subjected to acetone cleaning. The substrate temperature was controlled by a programmable temperature control unit and was measured by a Chromel-Alumel thermocouple placed onto dummy substrate. The distance between the source and the substrate was kept ~26cm. The thin film were deposited under high vacuum of 2×10^{-6} mbar and at the evaporation rate of 14 Å/s. Thickness of the films was kept around 50 nm or below measured in-situ by using a built-in quartz crystal thickness-monitor in the evaporation unit.

The resolution of TEM and HRTEM can be evaluated by lattice imaging of the standard Au nano particles. In the present study an attempt has been made to deposit highly stable Au nano particles using thermal evaporation technique to calibrate camera length/diffraction of Transmission electron microscope. NaCl, KCl crystal and carbon coated Ni and Cu grids were used as a substrate material. The films deposited onto KCl, crystal and carbon coated Cu TEM grids have been used for the microstructural investigations under HRTEM (make FEI, Technai G2 F30 STWIN). Compositional elemental analysis of the source material was carried out by using energy dispersive spectrometer (EDS) system attached to scanning electron microscope (SEM). Synthesis parameters have been optimized to grow uniformly distributed nanoparticles of Au. A detailed electron microscopy was carried out to record the images and corresponding selected area electron diffraction (SAED) patterns.

3 Results and Discussion

3.1 Elemental compositional analysis of source material

Before evaporating the source material (high purity gold wire) in the thermal evaporation process, elemental compositional analysis of the gold wire was carried out by using EDS which is an attachment of SEM. EDS spectra of the gold wire was used as the source material is represented in Fig. 5. From the EDS spectra revealed the presence of Au only, *i.e.*, no impurity. However some amount of atmospheric oxygen is also found to be present.

3.2 Particle shape and size analysis

In the present investigations efforts have been made to optimize the growth parameters to deposit nano structured thin films of gold on glass, KCl crystal and carbon coated copper TEM grids. The microstructural investigations of Au particle deposited on carbon coated Ni grids have been carried out to reveal the size, shape and separation between particles in the microstructure. Figure 6 shows the TEM micrograph of Au thin film deposited on KCl crystal and carbon coated TEM grids in the first attempt. TEM micrograph revealed the coalescence of gold nano particles separated by the channels (gap) as depicted in Fig. 6.

In the second attempt of thin films deposition care has been taken to control the deposition parameters such as quantity of the source material, distance between the evaporation boat and the substrate,

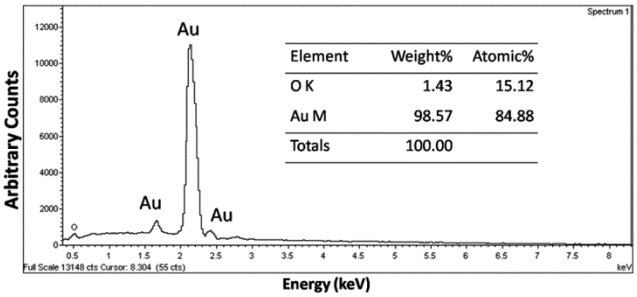

Fig. 5 — EDS spectra of the pure bulk gold wire.

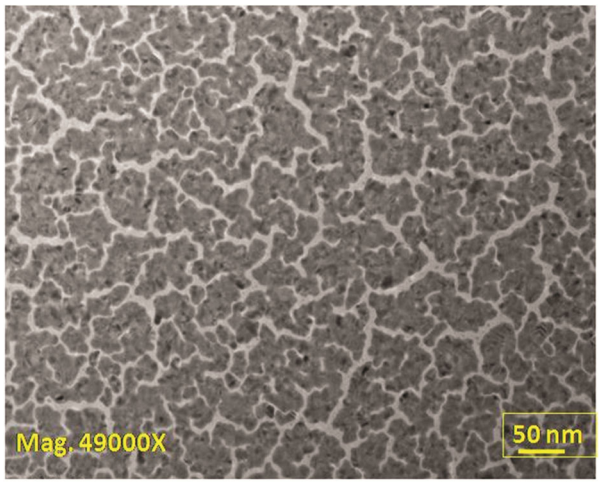

Fig. 6 — TEM image of Au thin film deposited on KCL crystal in the first attempt.

vacuum in the deposition chamber, time of deposition and temperature of the source material. Figure 7 shows the microstructural features associated with the thin film deposited in the second attempt. Microstructural features in this TEM image revealed that the gold nano particles are found to overlap on each other taking the shape of irregular dumble shape particles. Some individual particles are also seen spreading throughout the film.

In the third attempt, we have further controlled the deposition parameter and deposited the nanostructured thin film of gold on carbon coated copper/nickel grids and KCl crystal. Figure 8 shows TEM micrograph of the Au thin film recorded at 145000X magnification. TEM micrographs of the gold film exhibited uniform distribution of small nano-sized spherical and polyhedral shaped particles. The average particle size calculated from the electron micrograph was found to vary between 2 to 5 nm with inter-particle separation of 2 to 8 nm as depicted from the microstructure as shown in the figure. Microscopic features of the same areas of the film were further recorded at high magnification using HRTEM. The detailed microstructural features associated with the film is as depicted in Fig. 9 revealing lattice fringes in the individual particle. Interplaner spacing (d) as calculated from the TEM micrograph is found to be 1.44 Å. The calculated d spacing of the particular grain as marked in Fig. 9 was compared with the standard data of gold JCPDF file no. 04-0784 and found in the good agreement with the standard data.

SAED patter of the corresponding area recorded under TEM depicts the polycrystalline nature of the film. Diffraction pattern reveals the well resolved diffraction rings of polycrystalline gold. A set of important planes with *hkl* values 111, 200, 220, 311, 222, 400, 331, 420, and 422 of Au face centred cubic structure (lattice parameter a= 4.0786) are represented by strong and moderate intensity rings in electron diffraction pattern as depicted in Fig. 10.

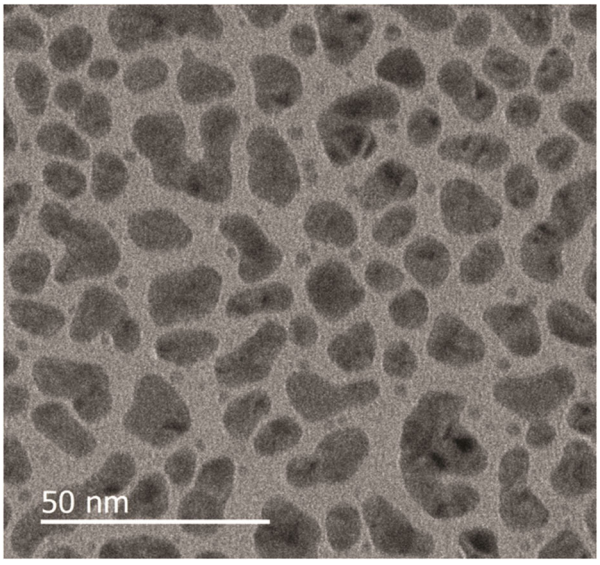

Fig. 7 — TEM image of Au thin film deposited on KCL crystal in the second attempt.

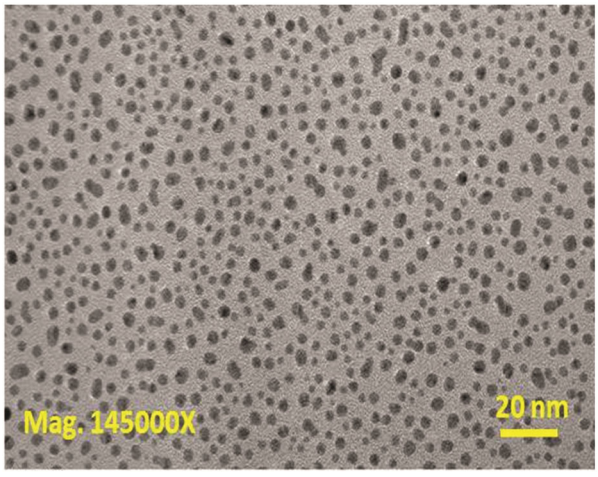

Fig. 8 — TEM image of Au thin film deposited on KCL crystal in the third attempt.

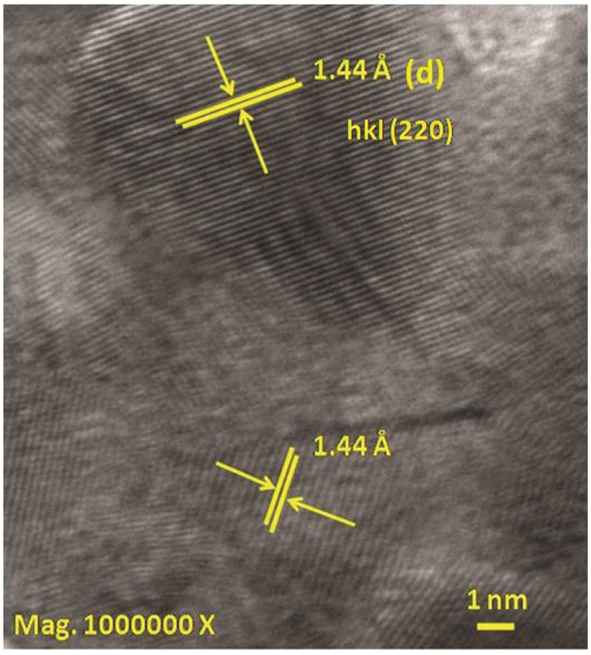

Fig. 9 — HRTEM image showing lattice fringes of Au with d - spacing 1.44 Å.

3.3 Calibration of camera length of TEM

We describe the magnification of the diffraction pattern by camera length L. This term arises from the X-ray projection diffraction camera which operates without lenses (because focusing of X-rays is very difficult). In this camera's magnification is increased by moving the recording film further away from the specimen. This principle can be applied in TEM.

If we increase the magnification of the lenses between specimen and the view screen, we increase the effective distance L between the specimen and the view screen.

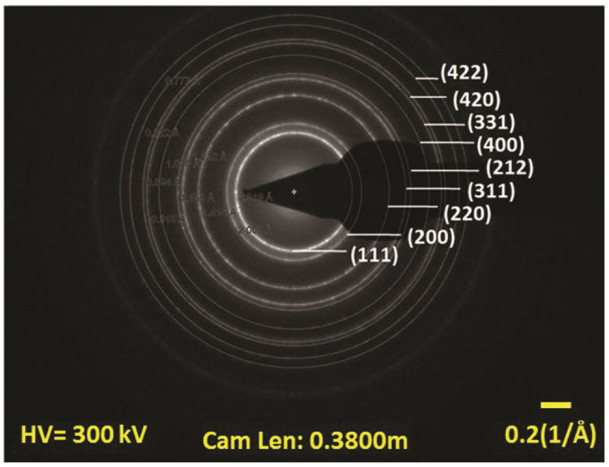

Fig. 10 — Selected area electron diffraction pattern of Au thin film showing polycrystalline nature of face centered cubic structure.

Electron micrographs and SAEDP of the same areas of the as deposited gold film were recorded under the microscope at suitable magnifications and camera length. Camera constant λL is determined by $2\times\lambda\times L = D\times d$ equation, where λ is the wave length of the incident electrons, L is the photographic plate to specimen distance, d is the interplaner spacing of the reflecting planes and $D=2r$, where r is the radial distance from centre of the transmitted beam spot to the diffracted beam spot (or ring) as shown in Fig. 4. Values of the camera constants were determined by measuring r from the diffraction pattern of a polycrystalline gold standard specimen (known d values). SAED pattern of gold particle is shown in Fig. 10.

On detailed analysis of the SAED pattern, some of the important planes with *hkl* values 111, 200, 220, 311, 222, 400, 331, 420, and 422 of Au face centred cubic structure (lattice parameter a= 4.0786) were observed represented by strong and moderate intensity rings in electron diffraction pattern in Fig. 10. The different rings of SAED pattern confirmed a polycrystalline random distribution of Au particles. The estimated d values are compared with the standard data of the gold specimen, shown in Table 2. From the table it is observed that these results are in good agreement with standard JCPDF file no. 04-0784. The calibration of the camera length (L) is done from time to time by recording the electron diffraction pattern of the standard gold sample using TEM.

Table 2 — Details of the diffraction rings

S. No.	Intensity of the ring	Observed d-values (Å)	Standard d-value JCPDF data (Å)	Observed *hkl* planes	Difference between observed and standard values (Å)
1.	S	2.319	2.356	111	0.037
2.	M	2.005	2.039	200	0.034
3.	M	1.416	1.442	220	0.026
4.	M	1.212	1.230	311	0.018
5.	W	1.158	1.177	222	0.019
6.	VVW	1.000	1.019	400	0.019
7.	W	0.918	0.936	331	0.018
8.	W	0.894	0.912	420	0.018
9.	W	0.822	0.833	422	0.011

*Note: S-Strong, M-Moderate, W- Weak, VVW- Very very weak

4 Conclusions

In the present investigations, efforts have been made to deposit good quality, stable, uniform and homogenous nano structured thin films of gold using thermal evaporation technique. Preliminary studies on the synthesis and characterization of nanostructured thin films prepared by thermal evaporation technique under high vacuum conditions resulted in uniformly distributed polycrystalline films. Synthesis parameters have been optimized to grow uniformly distributed nanoparticles of Au on carbon coated copper/Nickel grids and KCl/NaCl crystals. A detailed transmission electron microscopy was carried out to record the microstructural features associated and corresponding SAED patterns. Uniform Au nano-particles of round shape having the size between 2 to 5 nm are observed in electron microscopy images. Diffraction planes identified are (111), (200), (311) and (331) of Au matching with the standard JCPDF data. After optimizing the synthesis parameters, it is proposed to carry out inter laboratory calibration of the structural parameters of these films. Finally these nano structured thin will be utilized for calibrating the camera length, magnification and resolution of the TEM.

Acknowledgement

The present research work has been carried out under the CSIR Emeritus Scientist Scheme awarded to one of the authors SS. Authors are also thankful to Director CSIR - NPL to carry out the work and providing the characterization facilities.

References

1 Jia C L, Mi S B, Urban K, Vrejoiu I, Alexe M & Hesse D, *Nat* Mater, 7 (2008) 57.
2 Reimer L, *Transmission electron microscopy: Image formation and microanalysis*, 4th Edn, (Springer: Berlin), 1997.
3 Urban K W, *Science*, 321 (2008) 506.
4 McCaffrey J P & Baribeau J M, *Microsc Res Tech*, 32 (1995) 449.
5 Becker P, Bettin H, Danzebrink H U, Gl¨aser M, Kuetgens U, Nicolaus A, Schiel D, De Bi`evre P, Valkiers S & Taylor P, *Metrologia*, 40 (2003) 271.
6 Gao B & Kakimoto K, *J Cryst Growth*, 396 (2014) 7.
7 Möller H J, Funke C, Lawerenz A, Riedel S & Werner M, *Energy Mater Sol Cells*, 72 (2002) 403.
8 Yonemura M, Sueoka K & Kamei K, *Appl Surf Sci*, 130 (1998) 208.
9 Johnson C L, Snoeck E, Ezcurdia M, Rodríguez-González B, Pastoriza-Santos I, Liz-Marzán L M & H¨ytch M J, *Nat Mater*, 7 (2008) 120.
10 Guide to the Expression of Uncertainty in Measurement, (Intl Organization for Standardization (ISO) 1993, 1995.
11 Goncalves L M, Couto C, Alpuim P, Rolo A G, Völklein F & Correia J H, *Thin Solid Films*, 518 (2010) 2816.
12 Kim J H, Choi J Y, Bae J M, Kim M Y & Oh T S, *Mater Trans*, 54 (2013) 618.